

A Comparative Study of the Absolute-Magnitude Distributions of Supernovae

Dean Richardson, David Branch, Darrin Casebeer, Jennifer Millard, R. C. Thomas and E. Baron

Dept. of Physics and Astronomy, University of Oklahoma, Norman, OK 73019;
richards@nhn.ou.edu

ABSTRACT

The Asiago Supernova Catalog is used to carry out a comparative study of supernova absolute-magnitude distributions. An overview of the absolute magnitudes of the supernovae in the current observational sample is presented, and the evidence for sub-luminous and overluminous events is examined. The fraction of supernovae that are underluminous ($M_B > -15$) appears to be higher (perhaps much higher) than one fifth but it remains very uncertain. The fraction that are overluminous ($M_B < -20$) is lower (probably much lower) than 0.01. The absolute-magnitude distributions for each supernova type, restricted to events within 1 Gpc, are compared. Although these distributions are affected by observational bias in favor of the more luminous events, they are useful for comparative studies. We find mean absolute blue magnitudes (for $H_0 = 60$) of -19.46 for normal Type Ia supernovae (SNe Ia), -18.04 for SNe Ibc, -17.61 and -20.26 for normal and bright SNe Ibc considered separately, -18.03 for SNe II-L, -17.56 and -19.27 for normal and bright SNe II-L considered separately, -17.00 for SNe II-P, and -19.15 for SNe IIn.

Subject headings: supernovae: general — catalogs

1. Introduction

The absolute-magnitude distributions of the various supernova (SN) types provide vital information for determining SN rates, for advancing our knowledge of the stellar progenitors and their explosion mechanisms, and for planning future ground- and space-based SN searches. More than a decade ago, [MB90; mb90] used the Asiago Supernova Catalog ([?, the ASC;] barbon89) to carry out a comparative study of absolute-magnitude distributions. At the end of 1989, the ASC listed only 687 SNe, and many of those were of unknown type. By June, 2001 (updates are available at <http://merlino.pd.astro.it/~supern/>), the number of events in the ASC had increased to 1910. Almost all of the SNe of the 1990's had been assigned types, and some of the pre-1990 data had been improved. We therefore decided that an updated study of the absolute-magnitude distributions would be timely.

It should be acknowledged that the characteristic uncertainty of the apparent magnitudes listed in the ASC, perhaps 0.2 or 0.3 mag, is not negligible for this purpose. Thanks to the tremendous

interest in using SNe Ia as distance indicators for cosmology, studies of the SN Ia absolute-magnitude distribution now can be based on carefully selected samples of events for which both the apparent magnitudes and the relative distances are known to high accuracy (e.g., Hamuy 1996). The absolute-magnitude scatter in these samples can be further reduced in two ways. First, the host galaxy extinction can be taken into account for each SN using the SN's $B - V$ color. Next, the fact that some SNe Ia are intrinsically dimmer than others can be accounted for by using a correction to the light-curve width such as the Δm_{15} parameter (Phillips et al. 1999) or the method of multicolor light-curve shapes (MLCS; Riess 1996). With these corrections the dispersion in M_B for SNe Ia can be reduced to 0.11 (Phillips et al. 1999), making them extremely useful as distance indicators for cosmology.

Our present study, which has little to add to our knowledge of the SN Ia absolute-magnitude distribution, is directed more at the absolute-magnitude distributions of the other SN types. As far as the other SN types are concerned, either the number of events for which accurate peak apparent magnitudes have been reported remains small (SNe Ib, Ic, II-L, II-n) or the intrinsic dispersion in the peak absolute magnitude is large (SNe II-P). For these types a study such as this one, based on all available data, can be useful. For comparison with the other types, SNe Ia are included as well.

2. Data

Most of the SN types and apparent magnitudes are taken from the ASC (as of June, 2001). Several changes in the spectral types are made after examining spectra available to us. Some additional data (mostly for recent SNe Ia) are included from Perlmutter et al. (1999), Riess et al. (1999), Riess et al. (1998), Leonard et al. (2001), Clocchiatti et al. (2000), Macri et al. (2001), Matheson et al. (2000), van den Bergh (1994), Iwamoto et al. (2000) and Hatano et al. (2001). Magnitudes from Perlmutter et al. include K-corrections. Several changes in the apparent magnitudes are made after examining the Atlas of Light Curves of SNe I by Leibundgut et al. (1991). Where possible we use blue magnitudes. Photographic magnitudes are converted to blue magnitudes using the usual relation $B = m_{pg} + 0.3$. When necessary we assume that $B = V = R$ (except for the K-corrected events). The apparent magnitudes are corrected for Galactic extinction following Schlegel, Finkbeiner & Davis (1998) with the help of NED¹.

When possible, we use a Cepheid distance to the parent galaxy or to a member of the same galaxy group as the parent galaxy. The Cepheid distances are obtained from Freedman et al. (2001), Macri et al. (2001), Ferrarese et al. (2000) and Saha et al. (2001a,b). If a Cepheid distance is not available we use distances from the Nearby Galaxies Catalog (NGC; Tully 1988), which incorporates

¹The NASA/IPAC Extragalactic Database (NED) is operated by the Jet Propulsion Laboratory, California Institute of Technology, under contract with the National Aeronautics and Space Administration.

a Virgocentric infall model to relate galaxy recession velocity and distance. The errors in the relative distances to these events contribute significantly to the absolute-magnitude scatter in our figures. We rescale the distances from the $H_0 = 75 \text{ km s}^{-1} \text{ Mpc}^{-1}$ of the NGC to our choice of $H_0 = 60$.

If a Cepheid distance or an NGC distance is not available then the luminosity distance is calculated Kantowski, Kao & Thomas (2000), provided that the SN parent galaxy has a Galactocentric recession velocity of $cz > 2000 \text{ km s}^{-1}$. The luminosity distance is calculated assuming $H_0 = 60$, $\Omega_m = 0.3$, and $\Omega_\Lambda = 0.7$. Errors in the relative distances to these events should be small. A different choice of H_0 would simply rescale the absolute magnitudes. Different choices of Ω_m or Ω_Λ would change our plots only slightly (at large distances). A few SNe whose parent galaxies have $cz < 2000 \text{ km s}^{-1}$ but do not have a measured Cepheid distance and are not listed in the NGC are excluded from the study. The Large Magellanic Cloud, the site of SN 1987A, is assigned a distance modulus of 18.50.

3. Overview of Supernova Absolute Magnitudes

In Figure 1, absolute magnitude is plotted against distance modulus for all 297 SNe for which we have an estimate of the apparent magnitude at the time of maximum light; we will refer to these as *maximum-light* SNe. Also shown, at the left side of Figure 1, are estimates by Schaefer (1996) of the absolute magnitudes of six Galactic SNe of the last millennium that occurred within about 4 kpc of the Earth. Schaefer’s estimates actually are of M_V , rather than M_B , and his estimates of the distance moduli of these events range from 11.4 to 12.7, off-scale to the left of Figure 1. Figure 2 is like Figure 1, but for the 1078 SNe for which we have only lower limits to the peak absolute brightness because the apparent magnitude at the time of maximum light is unknown; we will refer to these as *limit* SNe. Both figures contain some straight lines to guide the eye. The horizontal line at $M_B = -19.5$ is regarded as characteristic of normal SNe Ia and we will refer to this as the SN Ia *ridge line*. The horizontal line at $M_B = -15$ and the vertical lines at $\mu = 30$ and $\mu = 35$ will be referred to below. The slanted lines correspond to apparent magnitudes of $B = 16$ and $B = 25$. Figure 1 shows that so far most of the maximum-light SNe have had peak apparent magnitudes brighter than $B = 16$, while Figure 2 shows that most of the limit SNe were fainter than $B = 16$ at their brightest observation. An indication of the dramatic observational progress that has taken place during the 1990s is that MB90 also plotted the $B = 16$ line, and only *four* maximum-light SNe were to the right of it. MB90 did not consider the limit SNe.

When viewing Figures 1 and 2 it is helpful to think in terms of several different distance regimes. First come the Galactic SNe, then SN 1987A and SN 1885A in the Local Group. Next come SNe in “nearby galaxies”, say within 10 Mpc ($\mu \leq 30$). The interval from $\mu = 30$ to $\mu = 35$ ($cz = 6000 \text{ km s}^{-1}$, 100 Mpc) includes many SNe of the Local Supercluster, with those of the Virgo cluster being concentrated near $\mu = 31.2$. From $\mu = 35$ (or less) to $\mu \simeq 40$ ($cz \simeq 60,000 \text{ km s}^{-1}$, $z \simeq 0.2$) is the “Hubble flow”, where luminosity distance depends on H_0 but only slightly on Ω_m .

and Ω_Λ . As will be seen below, most of the maximum-light events in the Hubble flow are SNe Ia; this is due to the observational bias in favor of luminous events. Beyond $\mu \simeq 40$ is the realm of the “high-redshift” SNe where, fortunately for cosmology, the luminosity distance depends significantly on Ω_m and Ω_Λ . Here too, most of the events are SNe Ia. At present most of the high-redshift events appear in Figure 2, as limit SNe, but some of these will become maximum-light SNe when their peak apparent magnitudes are eventually reported.

3.1. Subluminous Supernovae

SN 1987A stimulated interest in subluminous SNe, e.g., those having $M_B \geq -15$. The severe observational bias against them is obvious from Figures 1 and 2. Beyond $\mu = 30$, *none* of the maximum-light SNe are dimmer than $M_B = -15$. Schaefer (1996) considered two small volume-limited samples of SNe and concluded that a substantial fraction of all SNe are subluminous. One of his samples consisted of the six Galactic SNe that are represented in Figure 1. Two of the six are estimated to have been even less luminous than SN 1987A. Adopting these estimates, Hatano, Fisher & Branch (1997) carried out a Monte Carlo simulation of the visibility of Galactic SNe and concluded that it is quite likely that a significant fraction of the SNe in the Galaxy are “ultra-dim” ($M_V > -13$).

Schaefer’s other volume-limited sample consisted of SNe in nearby galaxies. In addition to SN 1987A there are four events in Figure 1 that have $M_B > -15$. SN 1940E (of unknown type) appeared in the dusty, nearly edge-on galaxy NGC 253 and probably was heavily extinguished so it may not have been intrinsically subluminous (Schaefer 1996). SNe 1923A and 1945B, both in the nearly face-on galaxy M83, do not appear to have been heavily extinguished (Schaefer 1996). SN 1973R, in NGC 3727, was observed to be quite blue (Patat et al. 1993) and therefore also is unlikely to have been heavily extinguished. It is likely that SNe 1923A (classified II-P only on the basis of its light curve), 1945B (unknown type), and 1973R (Type II-P) were intrinsically subluminous.

In Figure 1, among the Galactic SNe and the SNe in nearby galaxies having $\mu \leq 30$, seven of the 31 events are estimated to have had $M_B > -15$. Even this sample is by no means free of bias against subluminous events, so it appears that the fraction of all SNe that are subluminous is more than (possibly much more than) one fifth. But because the number of such events that have been seen is still so small, this fraction remains very uncertain.

3.2. Overluminous Supernovae

The data on maximum-light SNe that were available to MB90 showed no convincing evidence for events that were significantly overluminous with respect to the SN Ia ridge line, but by now it has become clear that overluminous events do exist, outstanding examples being the Type IIn

SN 1997cy (Germany et al. 2000; Turatto et al. 2000) at $M_B \leq -20.30$ and the peculiar Type Ic SN 1999as (Hatano et al. 2001) at $M_B \leq -21.60$.

In Figure 1, the two brightest SNe are well above the SN Ia ridge line, but the apparent magnitudes (and the types) of both are uncertain. The light curves of SNe 1955B (? , from)]zwicky56 and 1968A (? , mainly)]kaho68 are plotted and compared to a template light curve for SNe Ia by Leibundgut et al. (1991). Whether or not these two events were overluminous depends on the accuracy of the photographic photometry. It is not clear that either of these events were genuinely overluminous.

The peak apparent magnitudes for SN 1920A and SN 1963S given in the ASC would lead to $M_V = -22.2$ for both. However, the peak magnitudes were obtained by extrapolating well beyond the observations using the SN Ia template light curve (Leibundgut et al. 1991). Since both events are of unknown type, we treat them as limit SNe and use the observations without extrapolation to estimate the brightest apparent magnitudes. For SN 1920A we use $m_{pg} = 12.4$ (B. E. Schaefer 1999, private communication) and obtain $M_B = -20.40$, still overluminous. For SN 1963S we use $m_{pg} = 15.00$ (Haro 1964) and obtain $M_B = -20.97$, also overluminous.

In Figure 2, quite a few of the limit SNe have $M_B < -20$, but undoubtedly this is mainly because limit SNe were not as well observed as maximum-light SNe, so their magnitude errors tend to be larger. In particular, many of the apparent magnitudes of the high-redshift limit SNe are just first estimates that were made at the time of discovery; if and when more accurate apparent magnitudes are reported after the parent-galaxy light has been subtracted, most of them will come down to the SN Ia ridge line (because most of them are SNe Ia). The apparent magnitudes of nine of the most extreme cases in Figure 2, those that have $M_B \leq -21$ — SN 1999bd and 1961J (Type II); 1988O (Type Ia or Ic; see §4.1); 1984M (unknown type); 1995av and 2000ei (probable Type II); 2000eh and 1999fo (Type Ia); and SN 1971R (unknown type) — are the preliminary estimates reported in the IAU Circulars. We cannot be sure that any of these events really were overluminous, but it would take large magnitude errors to get them below $M_B = -20$.

At least two events in Figure 2, 1997cy and 1999as, were genuinely overluminous. Most of the others that appear to be overluminous in Figures 1 and 2 probably are spurious. In Figure 1, the fraction of the maximum-light events that have $M_B \leq -20$ is 0.067 (20 of 297). In Figure 2, the fraction is 0.101 (109 of 1078). In view of the luminosity bias and the tendency of apparent-magnitude errors to make ridge-line events appear to be overluminous, even the 0.067 is a generous upper limit to the true fraction of overluminous SNe. The true fraction probably is much lower than 0.01.

4. Absolute-Magnitude Distributions by Supernova Type

For the absolute-magnitude distributions we will consider only SNe that have $\mu < 40$ ($D < 1$ Gpc, $cz < 60,000$ km s⁻¹). This restriction is imposed because as Figure 1 shows, beyond $\mu = 40$

the luminosity bias is so severe that few events are much below the SN Ia ridge line. We need to keep in mind that even the distance-limited sample is strongly affected by luminosity bias — but to the extent that the bias is independent of the SN type, we can obtain some useful comparative results.

Histograms that appear in the following figures refer to absolute magnitudes that have been corrected only for Galactic extinction, not for extinction in the parent galaxy. In addition to considering the distributions of such uncorrected absolute magnitudes, we will also consider “intrinsic” distributions, obtained as follows. Hatano, Branch & Deaton (1998) used a Monte Carlo technique and a simple model of the spatial distributions of SNe and dust in a characteristic SN-producing galaxy to calculate extinction distributions for each SN type, averaged over all galaxy inclinations. Here, for each SN type, we assume for simplicity a Gaussian intrinsic absolute-magnitude distribution, convolve it with the appropriate extinction distribution from Hatano et al., and vary the mean absolute magnitude and dispersion of the intrinsic distribution to obtain the best fit to the uncorrected distribution, as determined by the Kolmogorov-Smirnov (K-S) test (Press et al. 1996). Because very few highly extinguished SNe make it into observational samples, we use the “extinction-limited subsets” of Hatano et al., which exclude extinctions larger than $A_B = 0.6$ mag. (Changing this value by ± 0.1 mag has very little effect on our results.) This simple statistical procedure makes a rough allowance for the effects of extinction on the absolute-magnitude distributions.

4.1. Type Ia

SNe Ia are plotted in Figure 3. Here, because of the relatively large amount of data available, SNe Ia whose apparent magnitudes were designated as uncertain in the ASC are treated as limit SNe. (For the other types discussed below, the number of events is smaller and/or the absolute-magnitude dispersion is large, so we accept those having uncertain apparent magnitudes as maximum-light SNe.)

In Figure 3, the maximum light SNe Ia do show a fairly high degree of concentration to the ridge line at $M_B = -19.5$, as expected. The scatter among the maximum-light events is due to a combination of intrinsically subluminal SNe 1991bg-like events, extinction in the parent galaxies, and errors in the apparent magnitudes and relative distances.

Some of the most extreme SN Ia are labeled in Figure 3. As mentioned above, the apparent magnitude of the very bright limit events SN 1988O, 1999fo and 2000eh are uncertain. Also, although 1988O is listed as a Type Ia in the ASC, from the published spectra (Stathakis & Sadler 1994) it is hard to exclude Type Ic. The five low-luminosity events that are labeled in Figure 3 include SNe 1991bg and 1957A, both of which are known to have been spectroscopically peculiar and intrinsically subluminal. SN 1986G is known to have been both spectroscopically peculiar and highly extinguished by dust in its parent galaxy. SNe 1996ai (Riess et al. 1999) and 1999cl

(Krisciunas et al. 2000) are thought to have been highly extinguished in their parent galaxies.

The histogram in Figure 4 shows the uncorrected M_B distribution for the 111 spectroscopically normal maximum-light SNe Ia that have $\mu \leq 40$. (If the spectroscopically low-luminosity events were included the distribution could not be represented by a gaussian.) Note that the distribution falls off steeply on the bright side, as expected if SNe Ia are thermonuclear disruptions of Chandrasekhar-mass white dwarfs (or mergers of two white dwarfs) because Type Ia light curves are powered by the radioactive decay of ^{56}Ni and its daughter ^{56}Co and there is a hard upper limit to the amount of ^{56}Ni that one (or two) exploding white dwarfs can eject. (This is a reason to suspect that SN 1988O was a Type Ic rather than a Type Ia.) The uncorrected distribution has a mean absolute magnitude of $\overline{M}_B = -19.16 \pm 0.07$, with a dispersion about the mean of $\sigma = 0.76$. The solid curve, the gaussian intrinsic distribution obtained as described above, has $\overline{M}_B = -19.46$, $\sigma = 0.56$. The extinction correction has made the mean absolute magnitude brighter by 0.3 mag., and produced a moderate reduction in the dispersion. The dashed curve is the convolution of the intrinsic distribution with the adopted extinction distribution; this is to be compared with the uncorrected distribution of the histogram. The K-S confidence level that the convolved distribution is consistent with the uncorrected distribution is 89%.

4.2. Types Ib and Ic

Figures 5 and 6 are like Figures 3 and 4, but for SNe Ibc (SNe Ib and Ic considered together because of the small amount of data available). In Figure 5, five maximum light SNe Ibc are significantly brighter than the others. The peculiar Type Ic SN 1998bw, well known for its possible connection to GRB980425, and the Type Ib SN 1954A are well observed. The peculiar Type Ib SN 1991D is listed as a limit in the ASC, but we have changed it to a maximum-light SN (S. Benetti et al., in preparation). For the Type Ib SN 1992ar we have used the average of two apparent magnitudes estimated by Clocchiatti et al. (2000) using two different template light curves for SNe Ic. The apparent magnitude of the Type Ic SN 1999cq is from Matheson et al. (2000).

The extremely bright limit event SN 1999as was discussed above. The apparent magnitudes of the other other bright limits, SNe 1999bz and 1993P (both Type Ic), are uncertain.

The uncorrected distribution of the 18 maximum-light SNe Ibc has $\overline{M}_B = -17.92 \pm 0.30$, $\sigma = 1.29$, and the intrinsic distribution has $\overline{M}_B = -18.04$, $\sigma = 1.39$. The K-S confidence level is 96% but the test tends to give overly high confidence levels when the sample size is small.

Figure 5 raises the suspicion that there may be two separate luminosity groups of SNe Ibc, one perhaps tightly clustered near $M_B \leq -19$ and another with a wider range at $M_B \simeq -17$. We will refer to these two groups as *bright* and *normal*. Because of this we have decided to consider a double peak distribution as well as the single peak distribution. The double peak distribution is

given by:

$$f(x) = f_0 \left(w \exp \left[-\frac{(x - x_1)^2}{2\sigma_1^2} \right] + \exp \left[-\frac{(x - x_2)^2}{2\sigma_2^2} \right] \right). \quad (1)$$

Here, x_1 and σ_1 are the mean absolute magnitude and dispersion, respectively, for the bright peak. The dim peak is similarly determined by x_2 and σ_2 . The fifth parameter is the weighting factor, w . (f_0 is the normalization constant.) All five of these parameters are varied to get the best fit.

Figure 7 is like Figure 6 but for a double peak distribution consisting of 5 bright and 13 normal SNe Ibc. For the normal group, the uncorrected distribution has $\overline{M}_B = -17.23 \pm 0.17$, $\sigma = 0.62$ and the intrinsic distribution has $\overline{M}_B = -17.61$, $\sigma = 0.74$. For the bright group, the uncorrected distribution has $\overline{M}_B = -19.72 \pm 0.24$, $\sigma = 0.54$ and the intrinsic distribution has $\overline{M}_B = -20.26$, $\sigma = 0.33$. The weight parameter for the intrinsic distribution is $w = 0.28$. The K-S confidence level approaches unity for these small samples.

The hydrogen-poor progenitors of SNe Ibc have small radii so the light curves of SNe Ibc are powered by the radioactive decay of ^{56}Ni . Since the rise times to maximum light of SNe Ibc and SNe Ia are similar, the ratio of the ejected masses of ^{56}Ni in SNe Ia and SNe Ibc is approximately given by the ratio of their peak luminosities. Using $M_B = -19.46$ for SNe Ia and $M_B = -18.04$ for SNe Ibc would give a ratio of nickel masses of 3.70, e.g., if the characteristic nickel mass of SNe Ia is $0.6 M_\odot$ then that of SNe Ibc would be $0.16 M_\odot$. However, SNe Ibc are redder than SNe Ia at maximum light and a smaller proportion of their luminosity goes into the B band (cf. MB90), therefore the $0.16 M_\odot$ may be an underestimate of the average value. The nickel mass determined from the tail of the light curve for SN 1994I was $0.07 M_\odot$ (Young, Baron & Branch 1995). Nickel masses for SNe Ibc may be strongly dependent on the nature of the progenitor.

4.3. Type II-L

SNe II-L are shown in Figures 8 and 9. For the whole sample of 16 maximum-light SNe II-L the uncorrected distribution has $\overline{M}_B = -17.80 \pm 0.22$, $\sigma = 0.88$ and the intrinsic distribution has $\overline{M}_B = -18.03$, $\sigma = 0.90$. The K-S confidence level is 91%.

All four of the bright SNe II-L — SNe 1961F, 1979C, 1980K, and 1985L — were well observed. As has been discussed by Young & Branch (1989), Gaskell (1992) and Patat et al. (1994) the available data suggest that it may be appropriate to divide SNe II-L into two luminosity groups; which, again, we refer to as bright and normal. When we do this, with only 4 events in the bright group and 12 in the normal group, we obtain Figure 10. For the normal group, the uncorrected distribution has $\overline{M}_B = -17.36 \pm 0.12$, $\sigma = 0.43$, and the intrinsic distribution has $\overline{M}_B = -17.56$, $\sigma = 0.38$. For the bright group, the uncorrected distribution has $\overline{M}_B = -19.12 \pm 0.12$, $\sigma = 0.23$, and the intrinsic distribution has $\overline{M}_B = -19.27$, $\sigma = 0.51$. The weight parameter for the intrinsic distribution is $w = 0.43$. For these small samples the confidence level, again, approaches unity.

If, as is commonly assumed, the progenitors of SNe II-L are red supergiants that have lost

much but not nearly all of their hydrogen envelopes, then the peak luminosities of SNe II-L depend primarily on the radius of the progenitor star and in some cases perhaps also on the strength of the circumstellar interaction, but not on the amount of ejected ^{56}Ni . If this is correct, then the similarity of the luminosities of the bright group of SNe II-L and the luminosities of normal SNe Ia ($\overline{M}_B = -19.27$ and -19.46 respectively), as well as the similarities of the bright and normal SNe II-L with the two possible groups of SNe Ibc, must be coincidental.

4.4. Type II-P

SNe II-P are shown in Figures 11 and 12. The uncorrected distribution of the 29 maximum-light SNe II-P has $\overline{M}_B = -16.61 \pm 0.23$, $\sigma = 1.23$. The intrinsic distribution has $\overline{M}_B = -17.00$, $\sigma = 1.12$ with a K-S confidence level approaching unity.

The progenitors of SNe II-P are red supergiants that have retained large hydrogen masses. The large dispersion in the luminosities of SNe II-P is primarily due to a wide range in the radii of the progenitor stars (Young 1994).

4.5. Type IIn

Figures 13 and 14 show SNe IIn. The brightest maximum-light event, SN 1983K, is listed as a Type II-P in the ASC but we have treated it as a Type IIn in view of the narrow lines in its spectra (Niemela, Ruiz & Phillips 1985). None of the maximum-light SNe IIn are extremely bright or dim. However, among the limit SNe there are four that are brighter than $M_B = -20$. SN 1997cy, discussed above, was genuinely overluminous, while the apparent magnitudes of the other three (SNe 1990S, 1995aa and 1999Z) are uncertain.

The uncorrected distribution of the 8 maximum-light SNe IIn has $\overline{M}_B = -18.78 \pm 0.31$, $\sigma = 0.92$, and the intrinsic distribution has $\overline{M}_B = -19.15$, $\sigma = 0.92$. The K-S confidence level approaches unity. SNe IIn are on average more luminous than other SNe II because of circumstellar interaction.

5. Summary

At least 7 of 31 SNe in our Galaxy and in galaxies within 10 Mpc appear to have been subluminal ($M_B \geq -15$). Considering that even in this sample there is an observational bias against them, it appears that more (perhaps much more) than one fifth of all SNe are subluminal, but because the number of such events seen so far is small, this fraction remains very uncertain.

Only 20 of 297 extragalactic maximum-light SNe appear to be overluminous ($M_B < -20$).

Considering the strong observational bias in favor of them, and that observational errors produce spuriously overluminous events, it is safe to conclude that the fraction of all SNe that are overluminous must be much lower than 0.01.

The results of our comparative study of the absolute-magnitude distributions of SNe in the distance-limited sample ($\mu < 40$) are summarized in Table 1. The main differences between our results and those of MB90 are that (1) it has become clear that overluminous SNe ($M_B \leq -20$) exist; (2) the absolute-magnitude dispersion of SNe Ibc has increased due to the discovery of some rather luminous events; and (3) we present results for SNe IIn, which on average are the most luminous type of core-collapse SNe.

Even though the SN discovery rate increased dramatically in the 1990's, the numbers of subluminal events, overluminous events, SNe II-L, SNe Ibc, and SNe IIn for which apparent magnitudes at maximum light are available are still small — this is especially so if SNe II-L and Ibc should be divided into two luminosity groups. Except for SNe Ia and II-P, the study of SN absolute-magnitude distributions remains data starved. Systematic programs of discovery and observation of events in the Hubble flow, such as the Nearby Supernova Factory (Aldering et al. 2001) underway at the Lawrence Berkeley National Laboratory, should substantially improve the situation during the coming years.

REFERENCES

- Aldering, G., et al. 2001, Supernova Factory Webpage (<http://snfactory.lbl.gov>)
- Barbon, R., Cappellaro, E., & Turatto, M. 1989, A&AS, 81, 421
- Clocchiatti, A., et al. 2000, ApJ, 529, 661
- Ferrarese, F., et al. 2000, ApJS, 128, 431
- Freedman, W., et al. 2001, ApJ, 553, 47
- Gaskell, C. 1992, ApJ, 389, L17
- Germany, L., Reiss, D., Sadler, E., Schmidt, B., & Stubbs, C. 2000, ApJ, 533, 320
- Hamuy, M., et al. 1996, AJ, 112, 2408
- Haro, G. 1964, IAUC 1856
- Hatano, K., Fisher, A., & Branch, D. 1997, MNRAS, 290, 360
- Hatano, K., Branch, D., & Deaton, J. 1998, ApJ, 502, 177
- Hatano, K., Branch, D., Nomoto, K., Deng, J. S., Maeda, K., Nugent, P., & Aldering, G. 2001, A&AS, 198, 3902
- Iwamoto, K., et al. 2000, ApJ, 534, 660
- Kaho, S. 1968, Tokyo Astr. Bull. 189, 2213
- Kantowski, R., Kao, J., & Thomas, R.C. 2000, ApJ, 545, 549
- Krisciunas, K., Hastings, N.C., Loomis, K., McMillan, R., Rest, A., Riess, A., & Stubbs, C. 2000, ApJ, 539, 658
- Leibundgut, B., Tammann, G., Cadonau, R., & Cerrito, D. 1991, A&AS, 89, 537
- Leonard, D., et al. 2001, ApJ, 553, 861
- Macri, L., Stetson, P., Bothun, G., Freedman, W., Garnavich, P., Jha, S., Madore, B., & Richmond, M. 2001, ApJ, Submitted (astro-ph/0105491)
- Matheson, T., Filippenko, A., Chornock, R., Leonard, D., & Li, W. 2000, AJ, 119, 2303
- Miller, D., & Branch, D. 1990, AJ, 100, 2
- Niemela, V.S., Ruiz, M.T., & Phillips, M.M. 1985, ApJ, 289, 52
- Patat, F., Barbon, R., Cappellaro, E., & Turatto, M. 1993, A&AS, 98, 443

- Patat, F., Barbon, R., Cappellaro, E., & Turatto, M. 1994, *A&A*, 282, 731
- Perlmutter, S., et al. 1999 *ApJ*, 517, 565
- Phillips, M., Lira, P., Suntzeff, N., Schommer, R.A., Hamuy, M., & Maza, J. 1999 *AJ*, 118, 1766
- Press, W., Teukolsky, S., Vetterling, W., & Flannery, B. 1996, *Numerical Recipes* (2d ed.; Cambridge: Cambridge University Press)
- Riess, A., Press, W., & Kirshner, R. 1996, *ApJ*, 473, 88
- Riess, A., et al. 1998, *AJ*, 116, 1009
- Riess, A., et al. 1999, *AJ*, 117, 707
- Saha, A., Sandage, A., Thim, F., Labhardt, L., Tammann, G., Christensen, J., Macchetto, F., & Panagia, N. 2001a, *ApJ*, 551, 973
- Saha, A., Sandage, A., Tammann, G., Dolphin, A., Christensen, J., Panagia, N., & Macchetto F. 2001b, *ApJ*, Submitted (astro-ph/0107391)
- Schaefer, B. E. 1996, *ApJ*, 464, 404
- Schlegel, D., Finkbeiner, D., & Davis, M. 1998, *ApJ*, 500, 525
- Stathakis, R. A., & Sadler, E. M. 1994, *Proc. Astron. Soc. Austr.*, 11, 1
- Tully, R. B. 1988, *Nearby Galaxies Catalog* (Cambridge: Cambridge University Press)
- Turatto, M., et al. 2000, *ApJ*, 534, 57
- van den Bergh, S. 1994, *ApJS*, 92, 219
- Young, T., & Branch, D. 1989, *ApJ*, 342, L79
- Young, T. 1994, PhD Thesis, The University of Oklahoma
- Young, T., Baron, E., & Branch, D. 1995, *ApJ*, 449, L51
- Zwicky, F. 1956, *PASP*, 68, 271

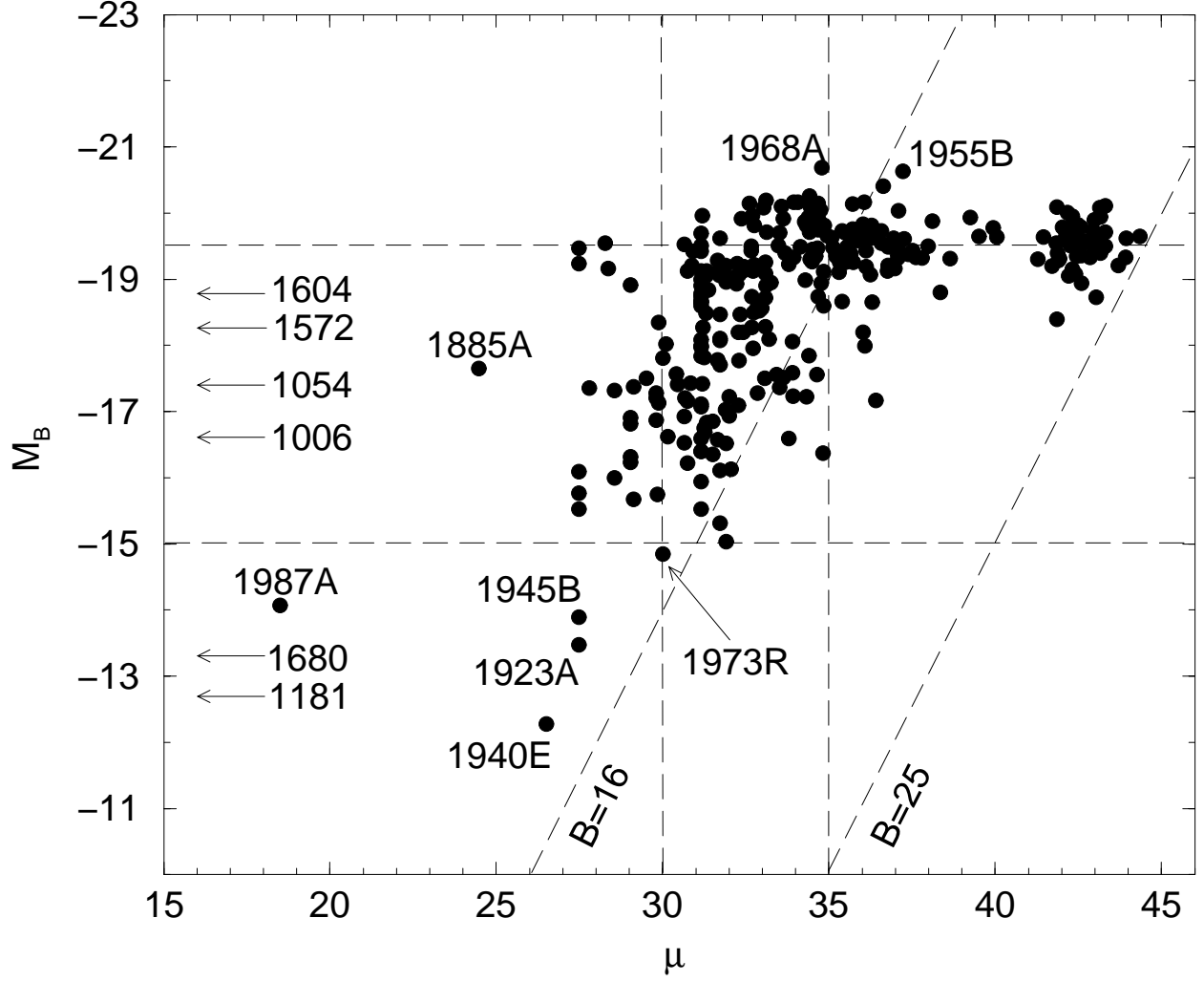


Fig. 1.— Absolute magnitude is plotted against distance modulus for all 297 maximum-light SNe, regardless of type.

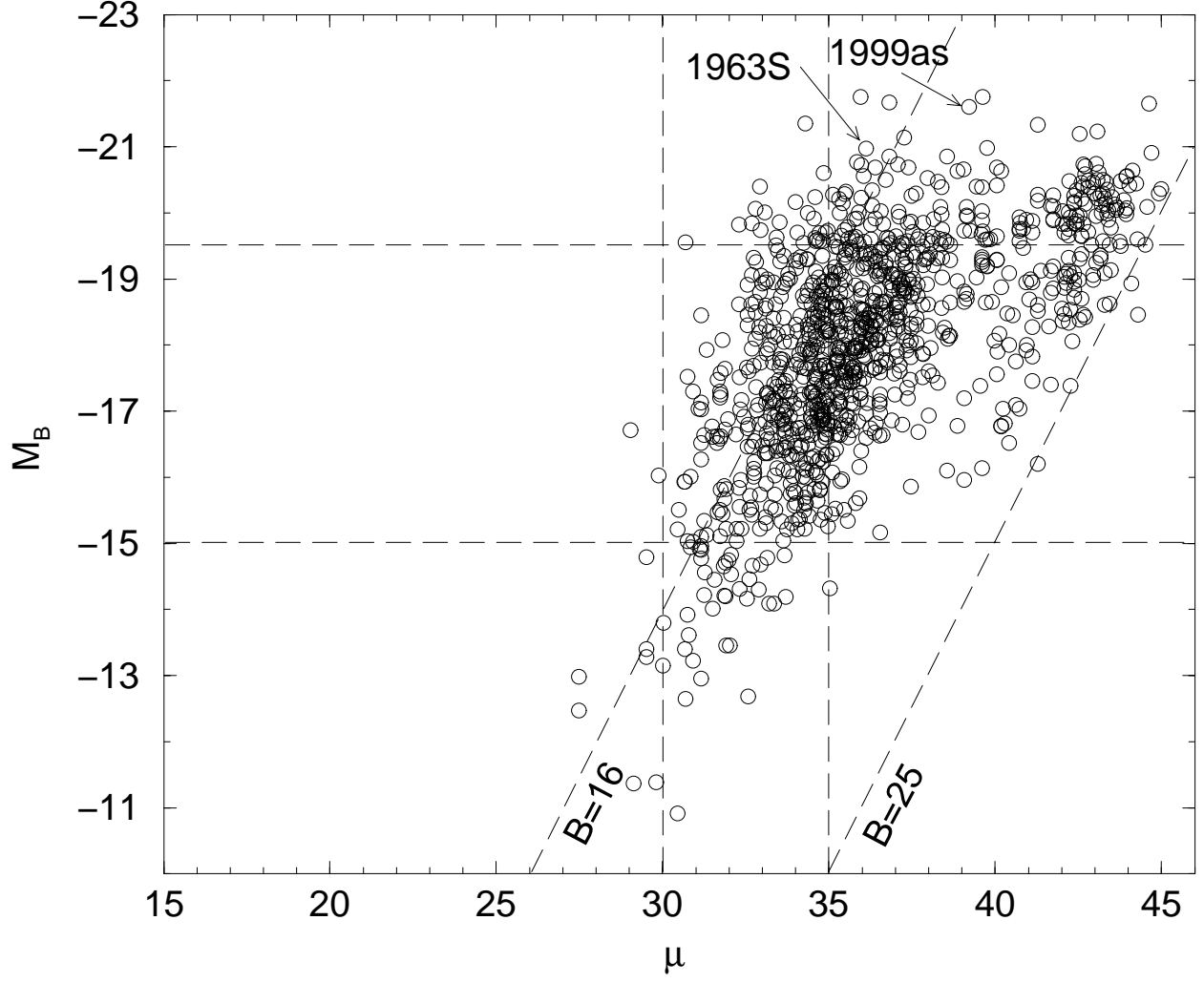


Fig. 2.— Absolute magnitude is plotted against distance modulus for all 1078 limit SNe, regardless of type.

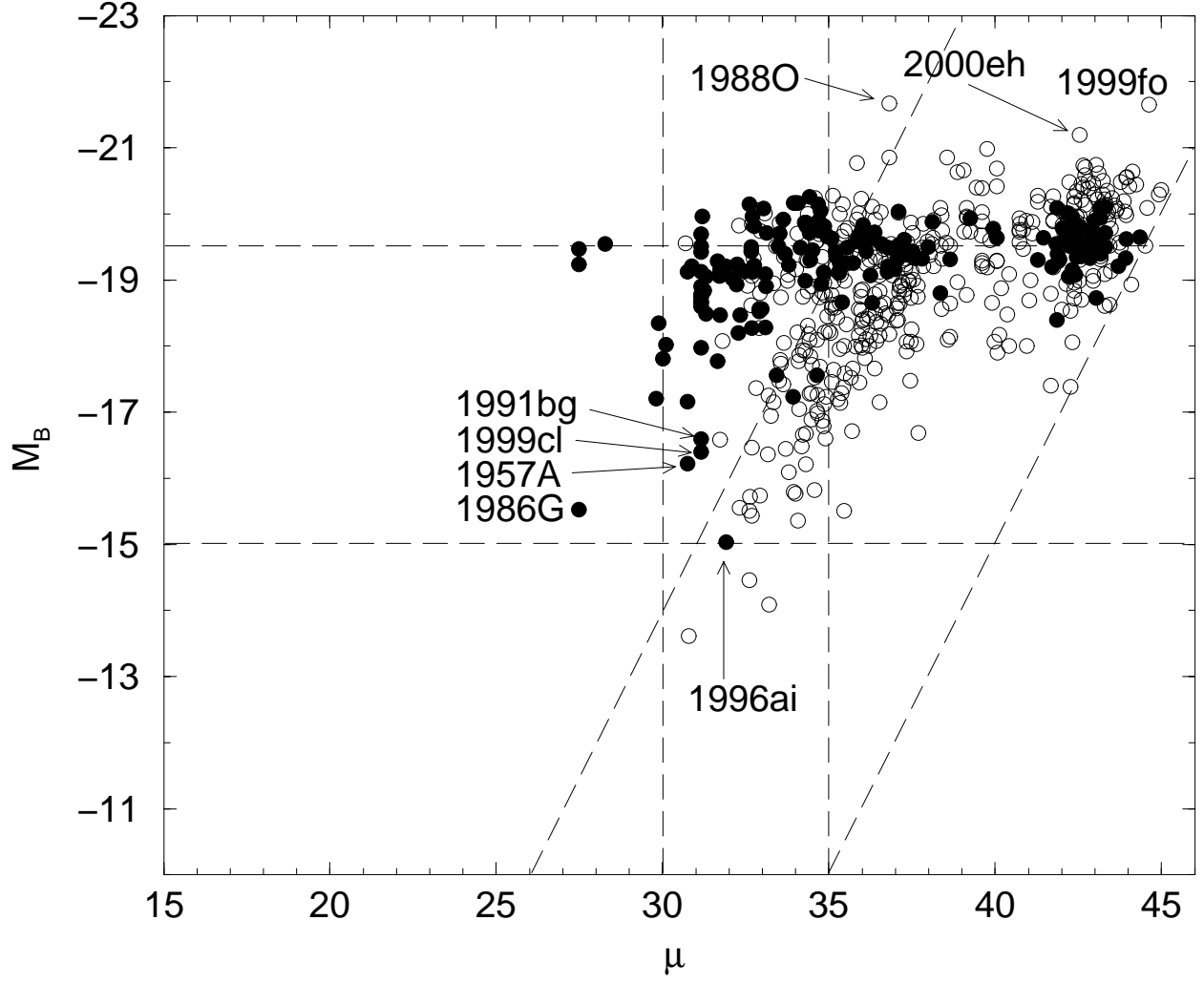


Fig. 3.— Absolute magnitude is plotted against distance modulus for SNe Ia. Filled symbols are maximum-light SNe (174) and open symbols are limit SNe (395).

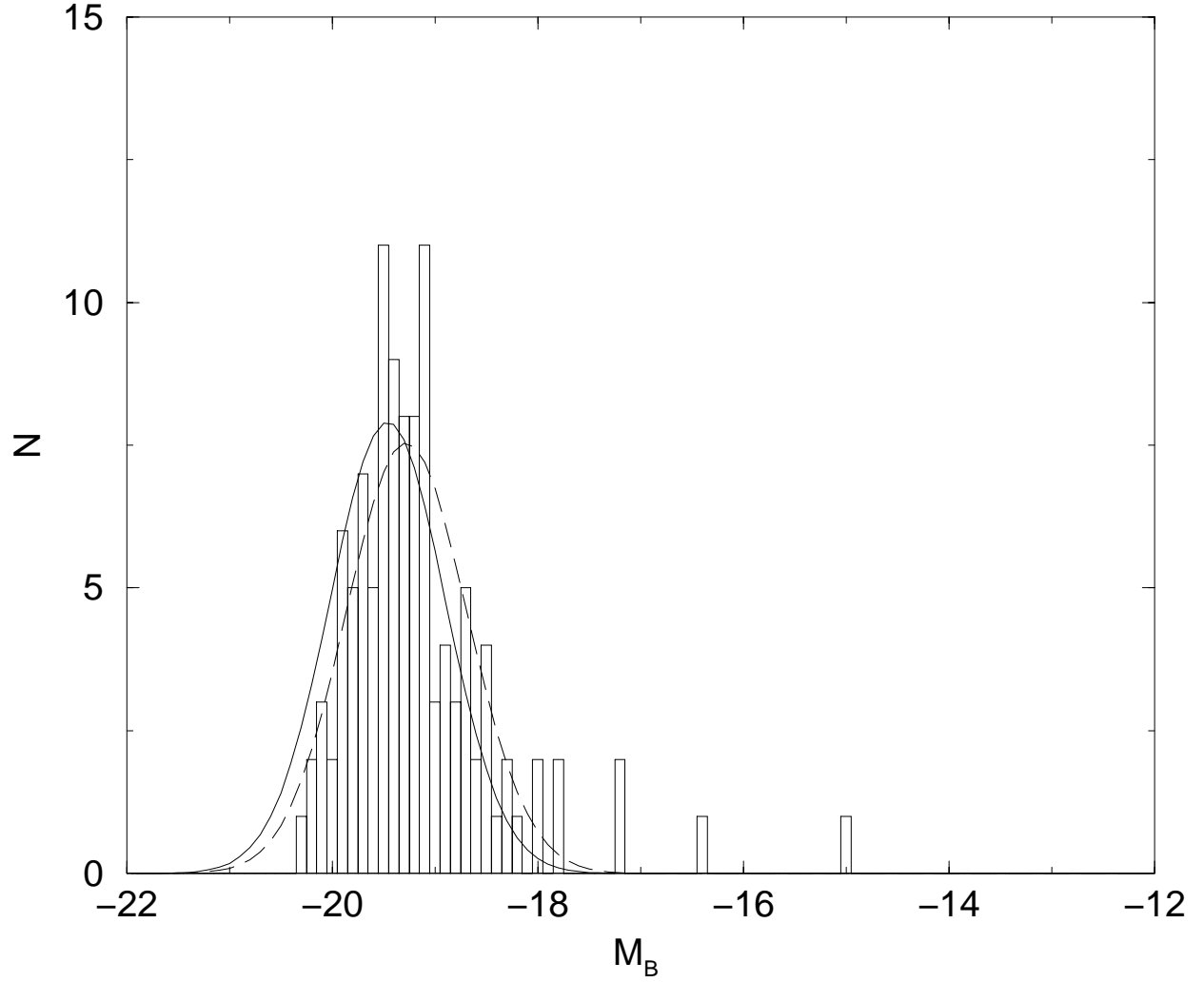


Fig. 4.— The absolute-magnitude distribution of 111 normal SNe Ia at maximum-light having $\mu \leq 40$, uncorrected for extinction in the parent galaxies (histogram) is compared with the convolution (dashed line) of the adopted intrinsic gaussian distribution (solid line) with the adopted parent-galaxy extinction distribution (see text).

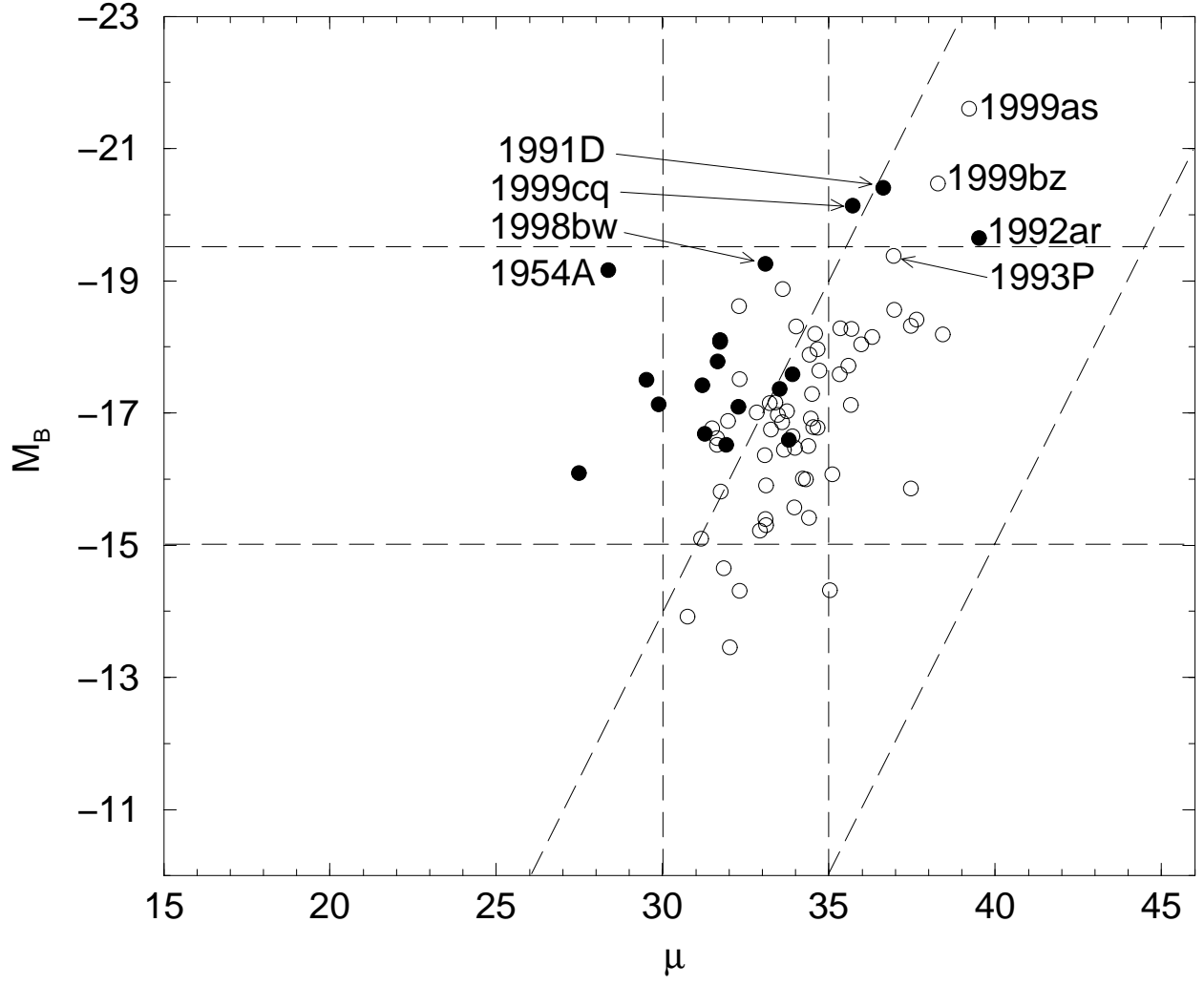


Fig. 5.— Like Figure 3 but for SNe Ibc. (18 maximum-light SNe and 59 limit SNe.)

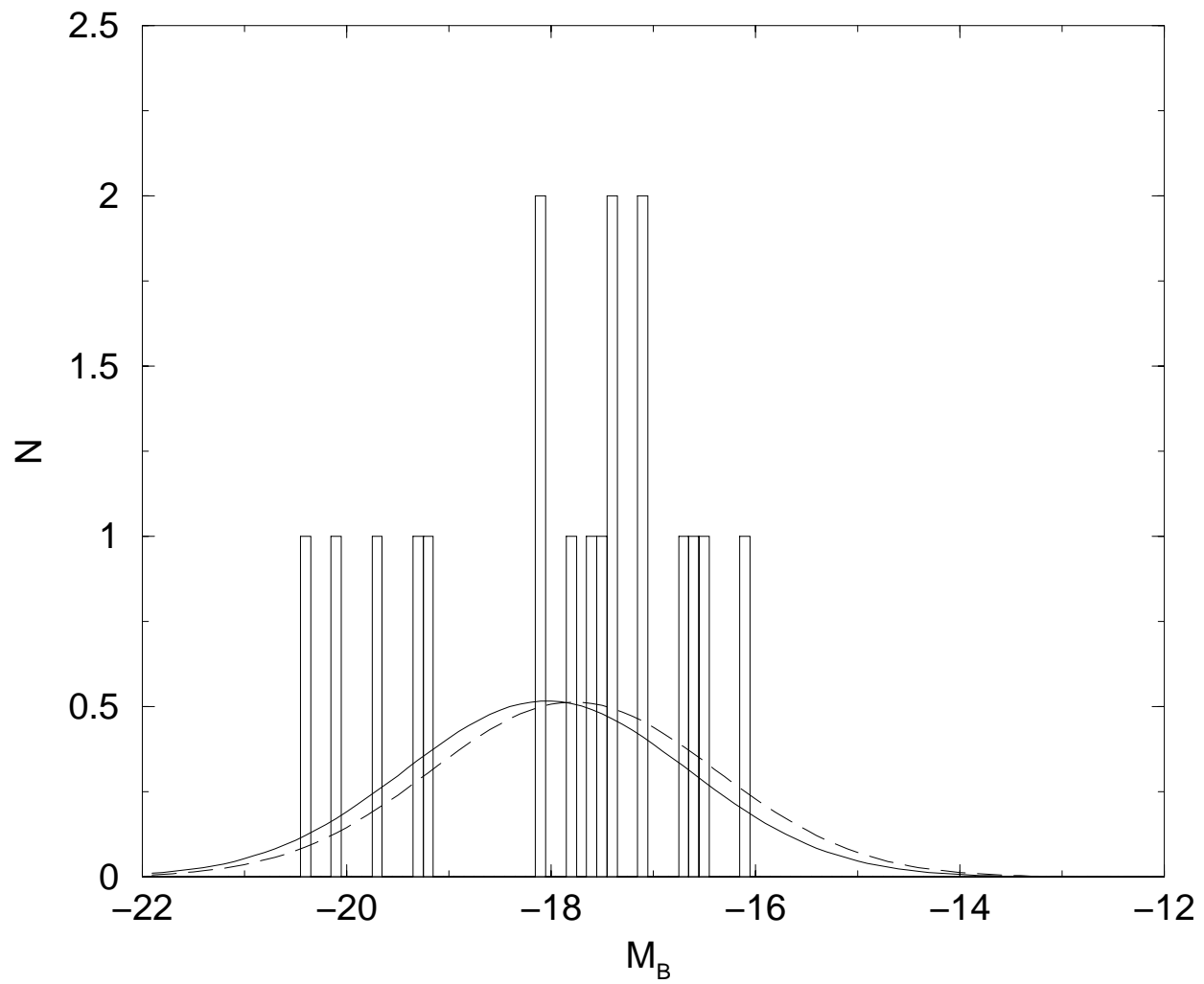


Fig. 6.— Like Figure 4 but for 18 SNe Ibc.

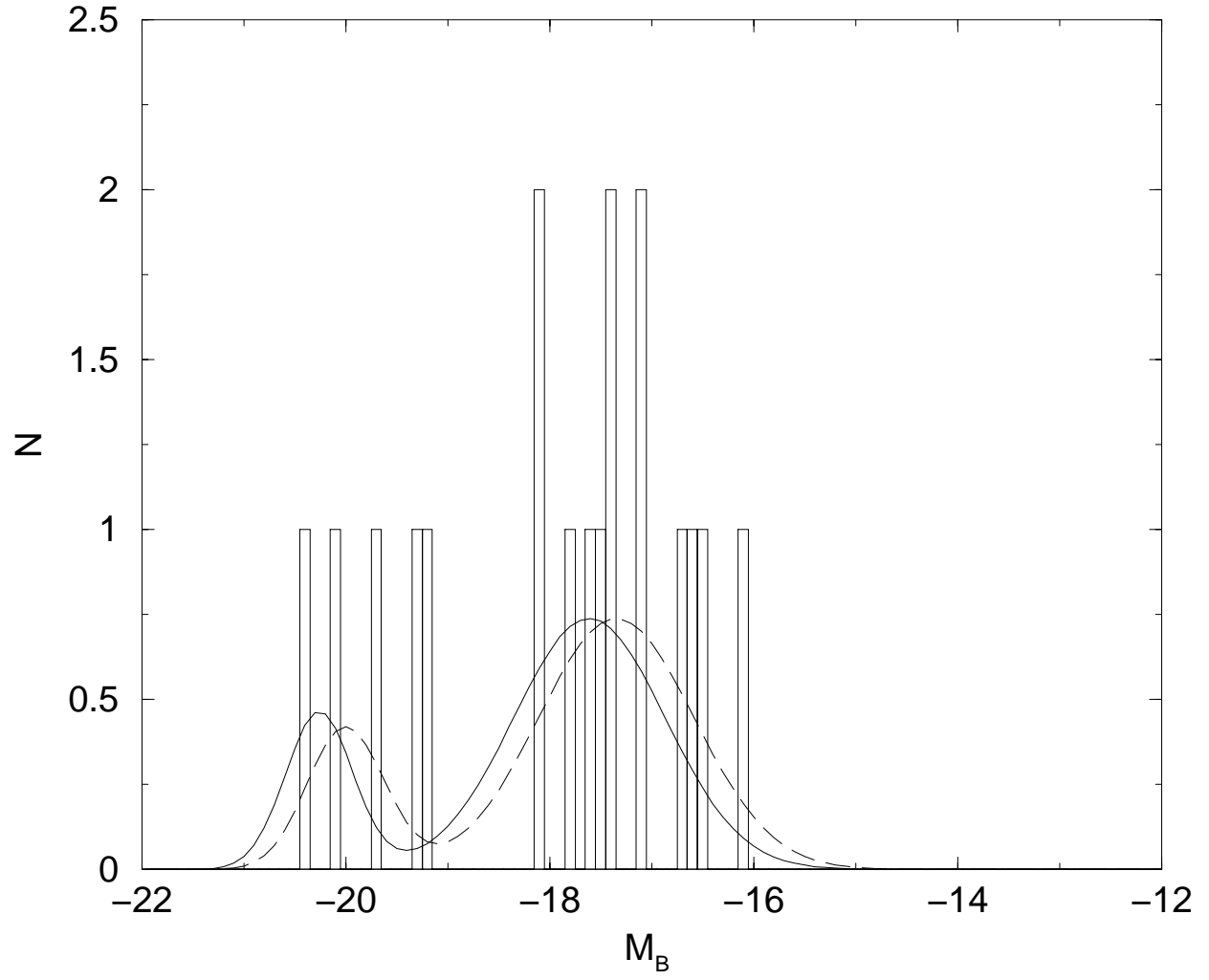


Fig. 7.— Like Figure 6 but for SNe Ibc divided into two groups of 5 bright and 13 normal events.

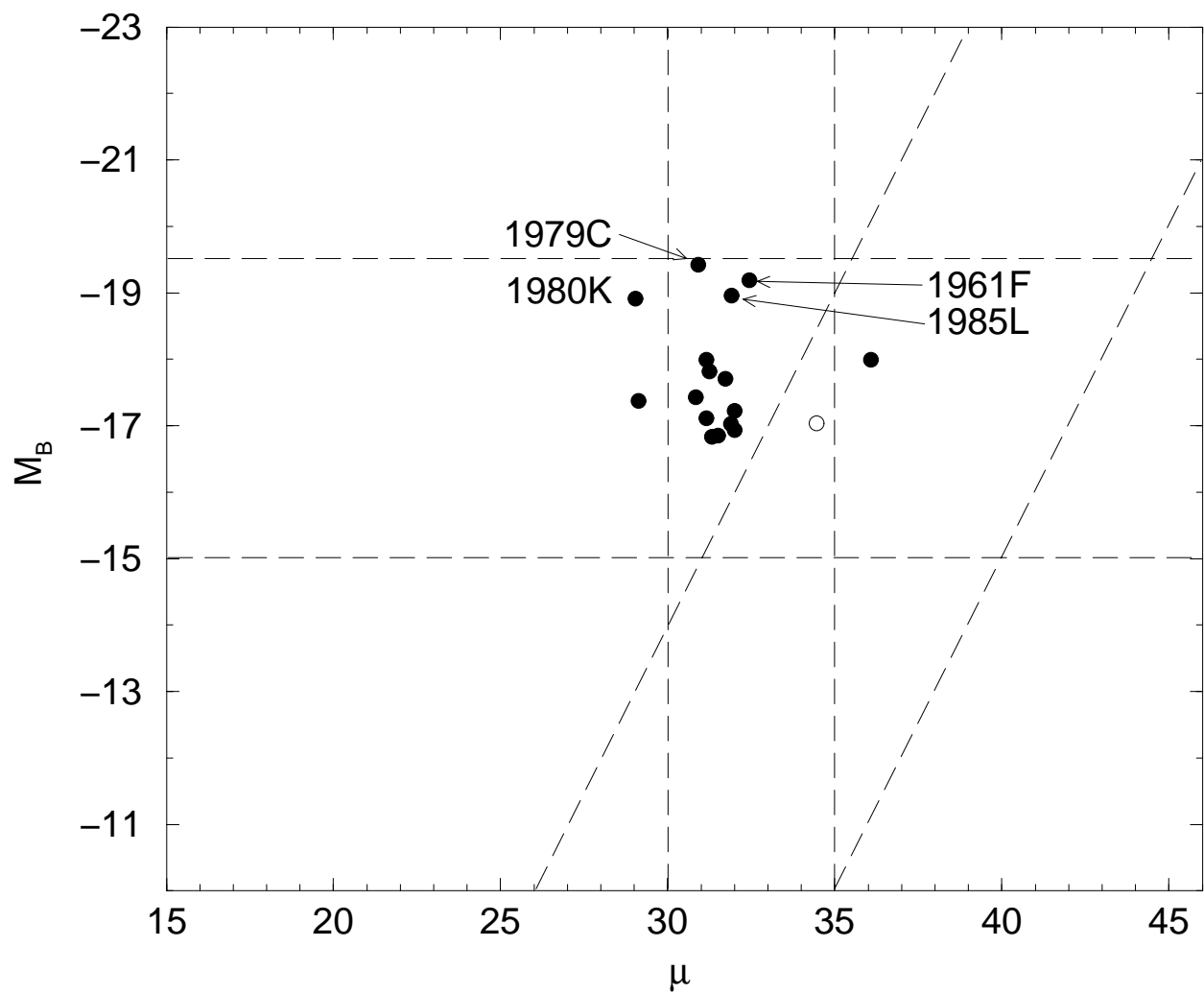


Fig. 8.— Like Figure 3 but for SNe II-L. (16 maximum-light SNe and 1 limit SN.)

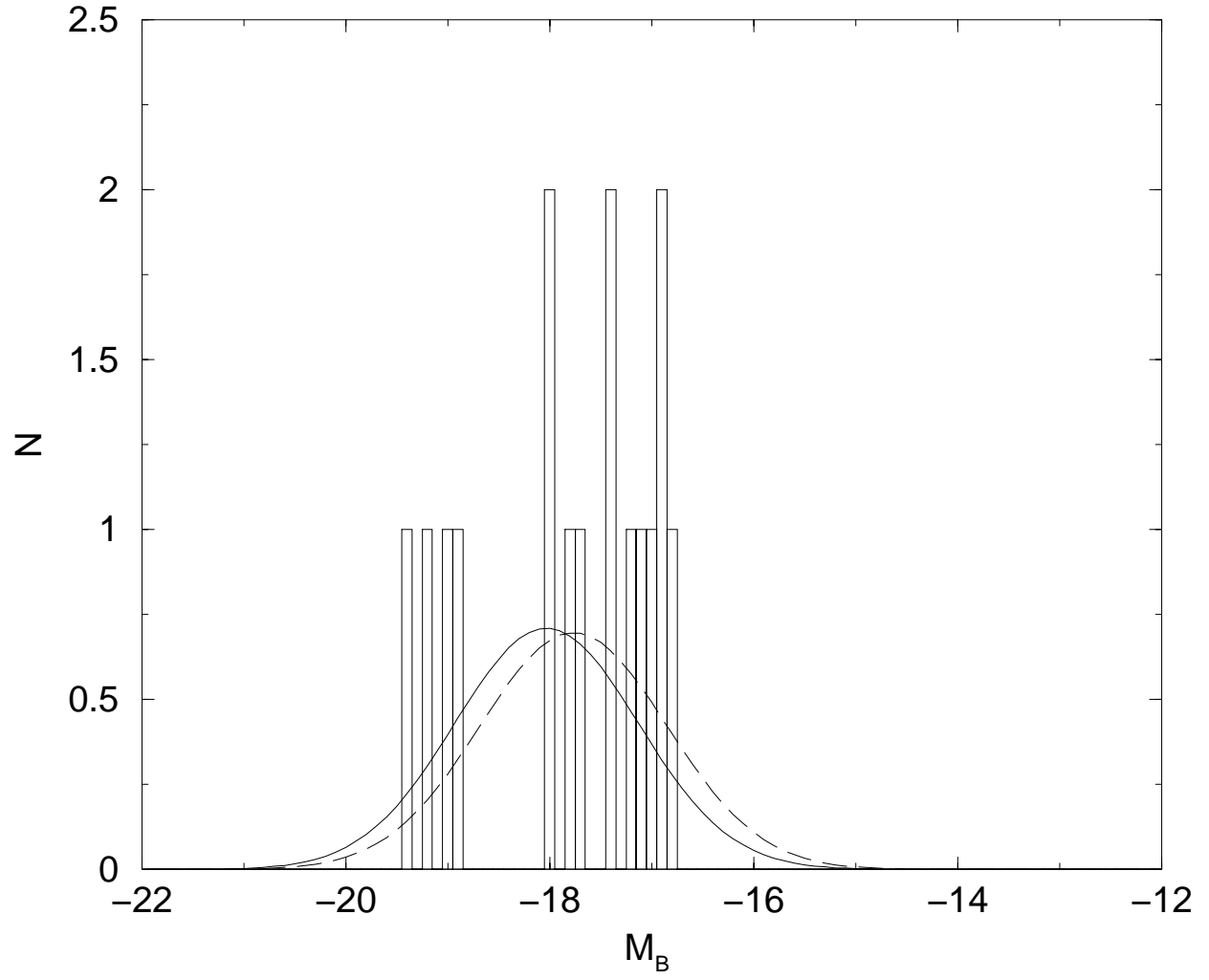


Fig. 9.— Like Figure 4 but for 16 SNe II-L.

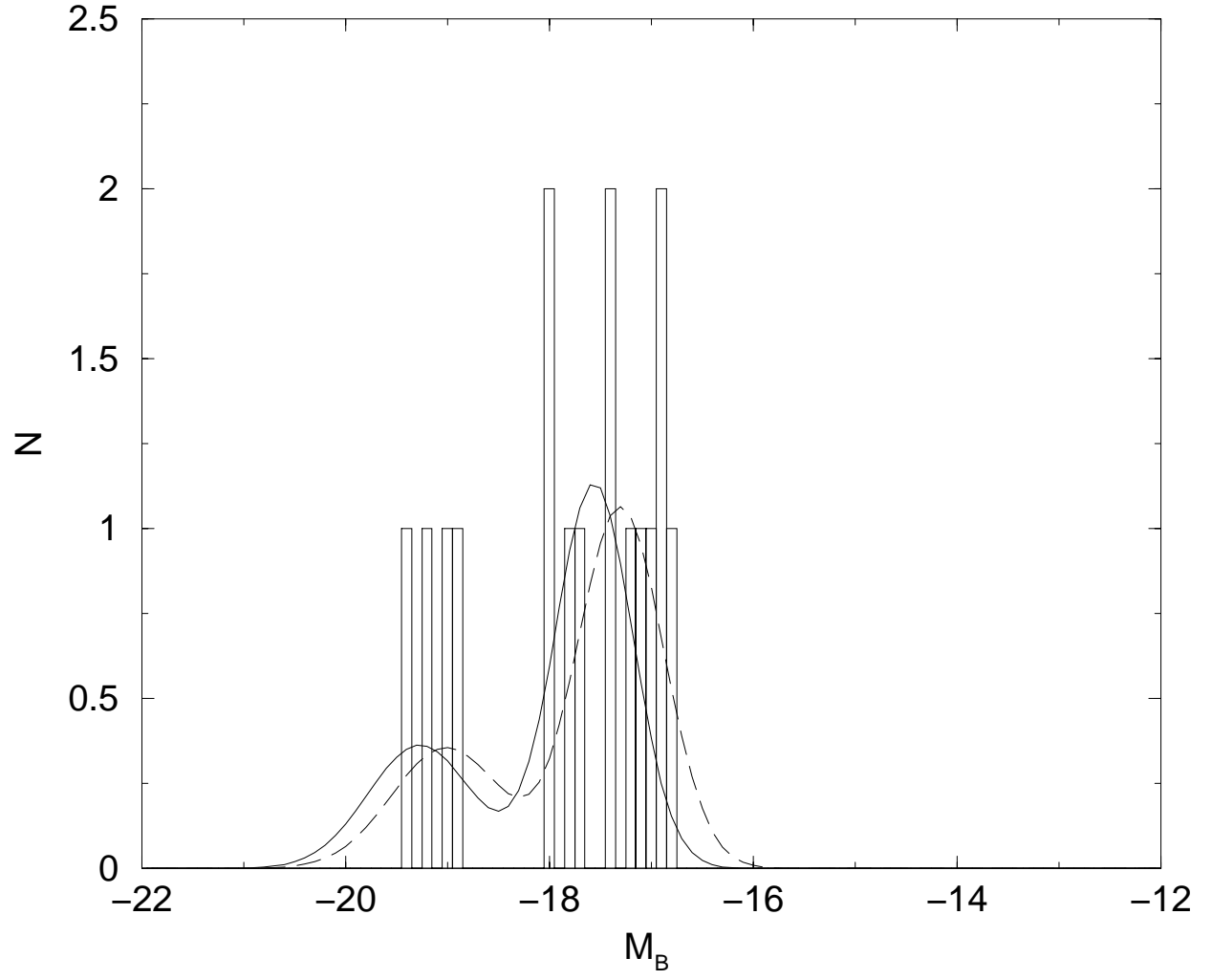


Fig. 10.— Like Figure 7 but for SNe II-L. (4 bright and 12 normal events.)

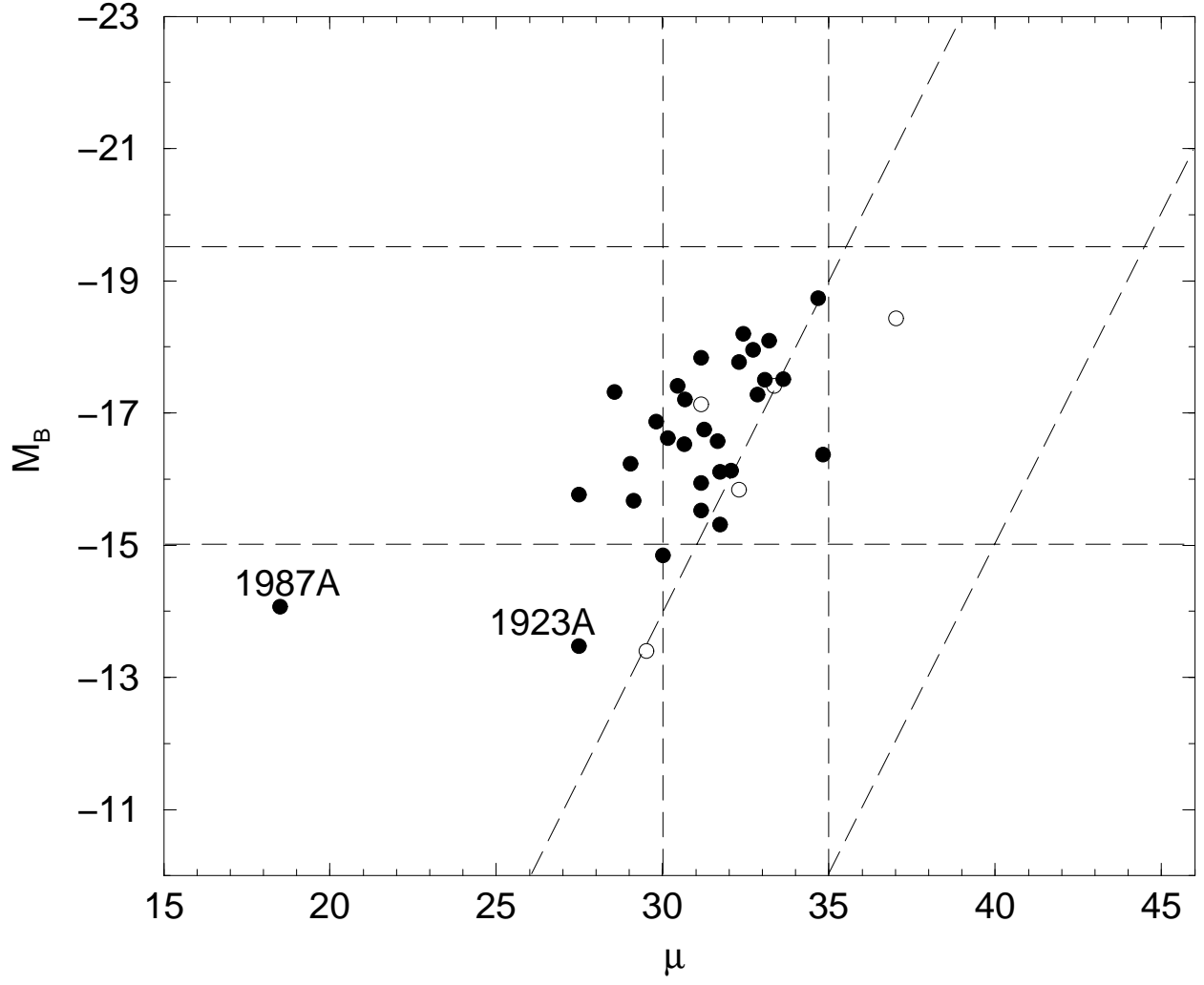


Fig. 11.— Like Figure 3 but for SNe II-P. (29 maximum-light SNe and 5 limit SNe.)

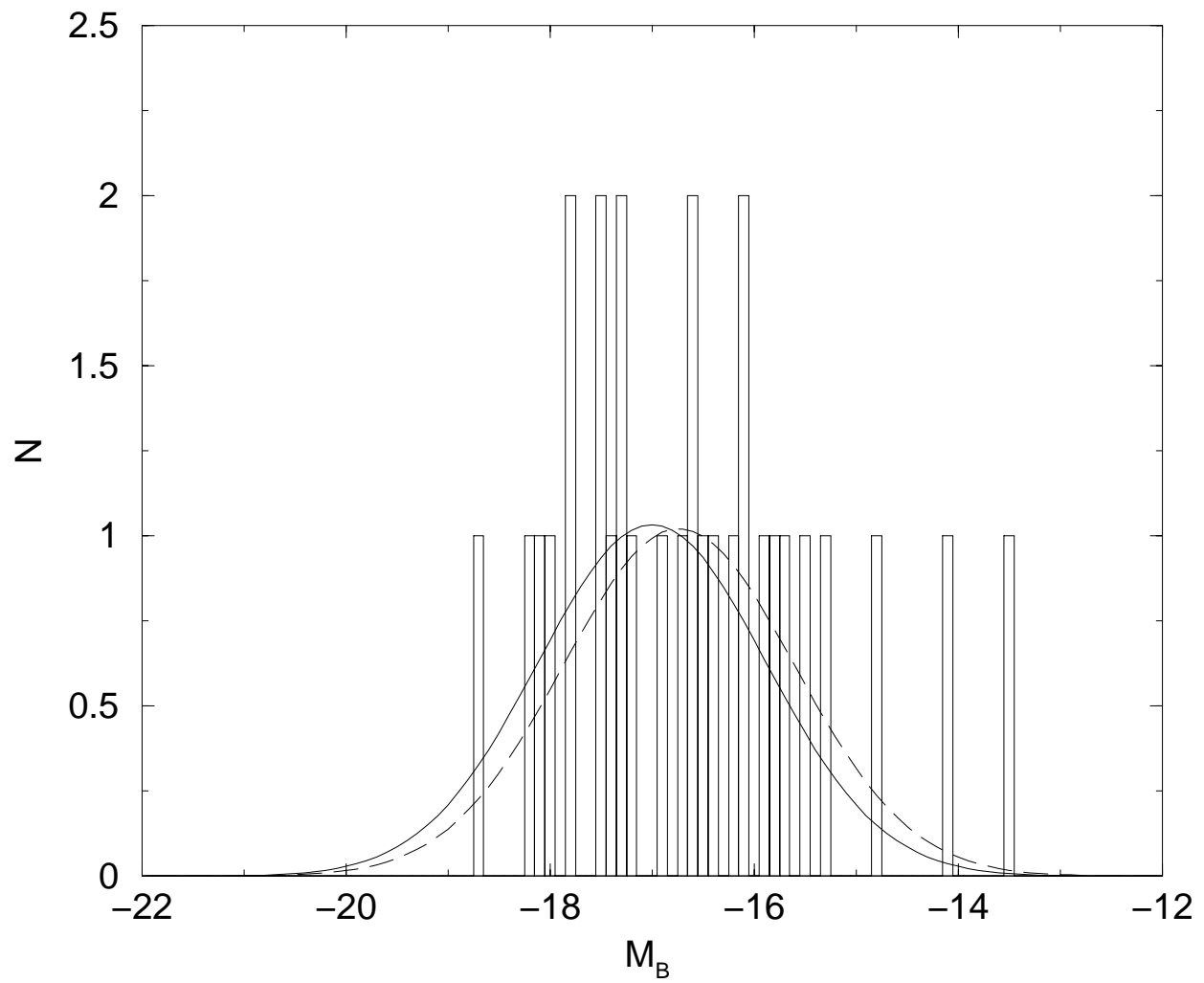


Fig. 12.— Like Figure 4 but for 29 SNe II-P.

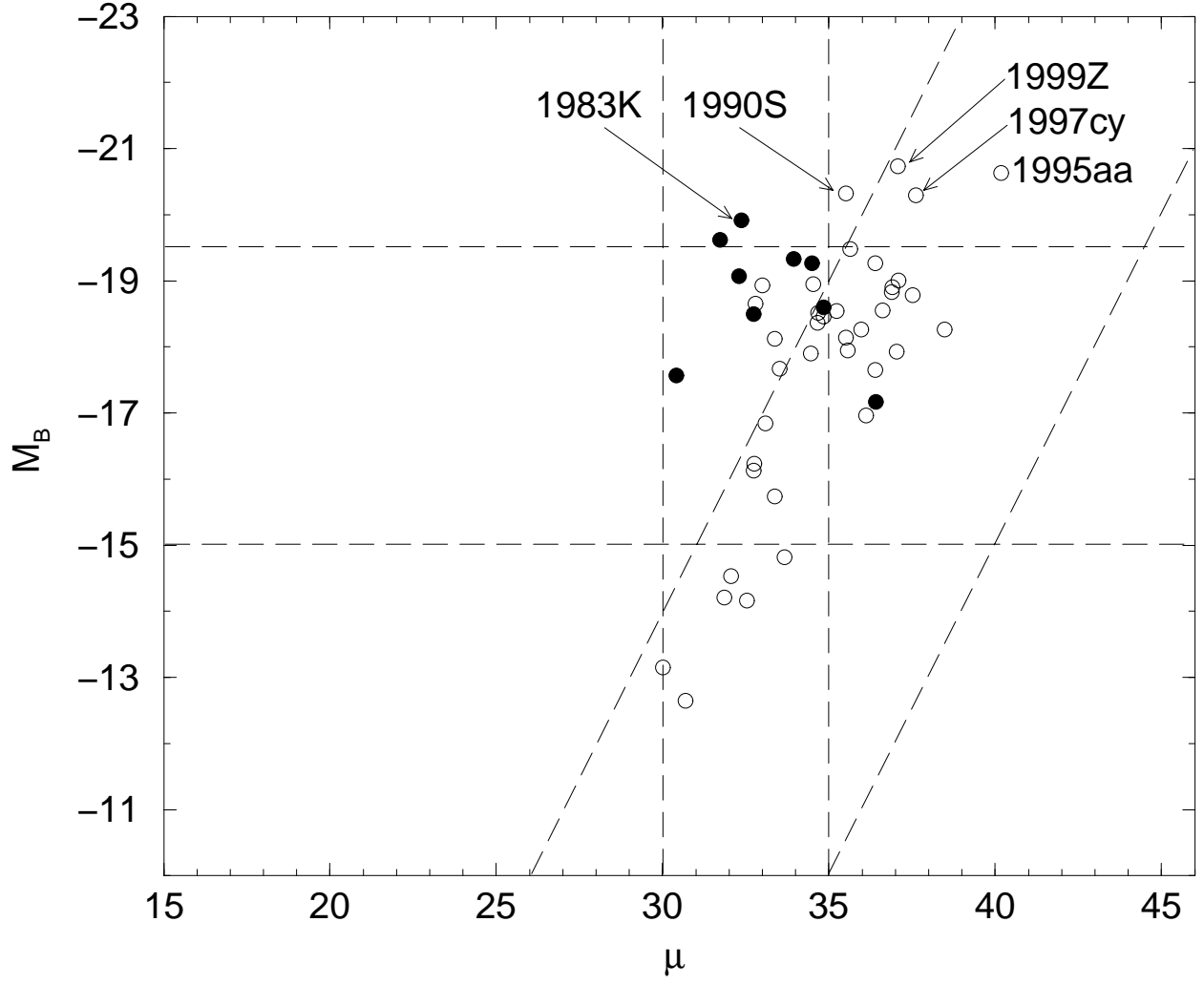


Fig. 13.— Like Figure 3 but for SNe II_n. (9 maximum-light SNe and 38 limit SNe.)

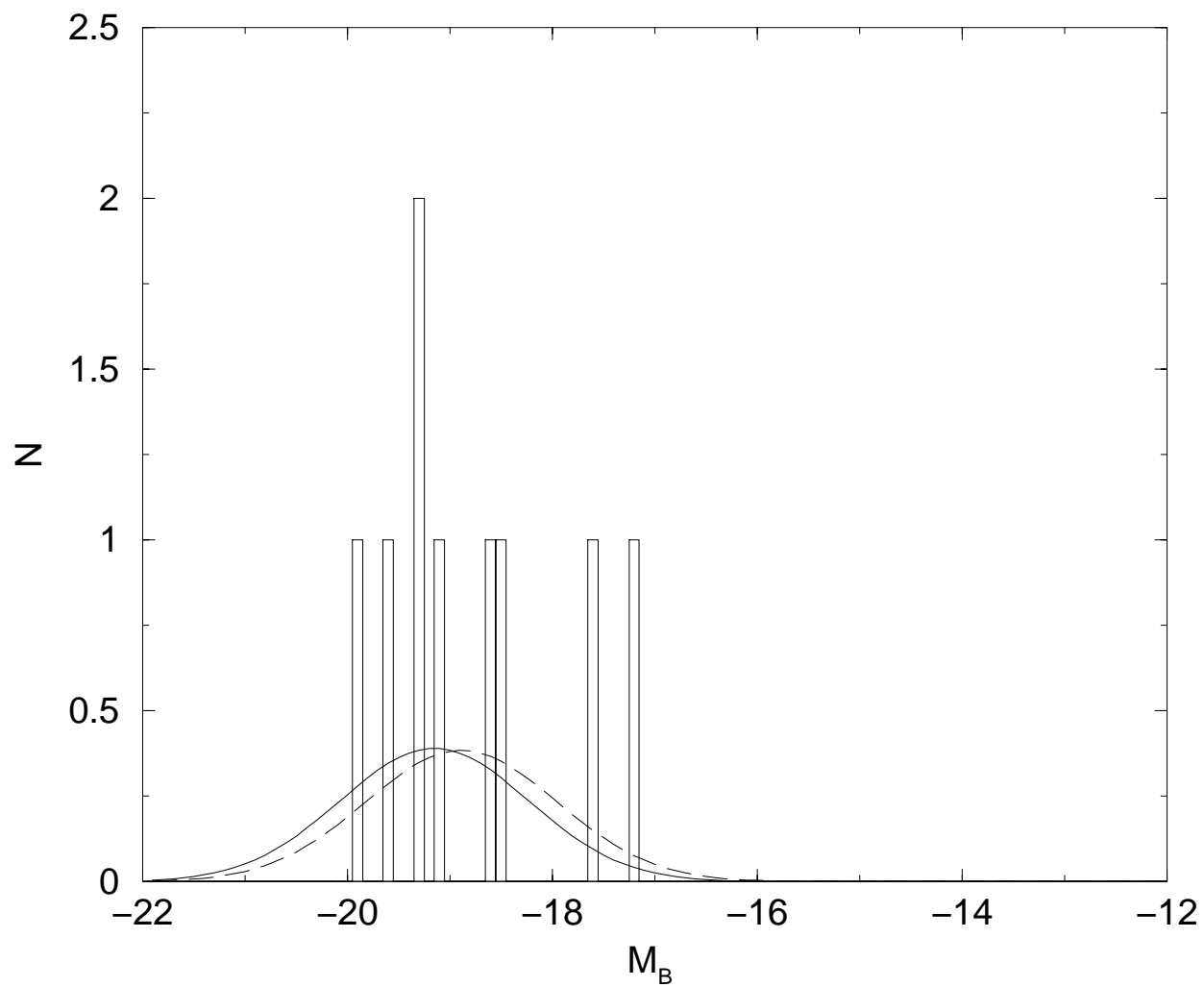


Fig. 14.— Like Figure 4 but for 9 SNe IIn.

Table 1. Results.

SN Type	$\overline{M}_{B,obs}$	σ_{obs}	$\overline{M}_{B,int}$	σ_{int}	Conf.	N
Normal Ia	-19.16 ± 0.07	0.76	-19.46	0.56	0.89	111
Total Ibc	-17.92 ± 0.30	1.29	-18.04	1.39	0.96	18
Bright Ibc	-19.72 ± 0.24	0.54	-20.26	0.33	~ 1	5
Normal Ibc	-17.23 ± 0.17	0.62	-17.61	0.74	~ 1	13
Total II-L	-17.80 ± 0.22	0.88	-18.03	0.90	0.91	16
Bright II-L	-19.12 ± 0.12	0.23	-19.27	0.51	~ 1	4
Normal II-L	-17.36 ± 0.12	0.43	-17.56	0.38	~ 1	12
II-P	-16.61 ± 0.23	1.23	-17.00	1.12	~ 1	29
IIn	-18.78 ± 0.31	0.92	-19.15	0.92	~ 1	9